Sciencexpress Reports

Revised 4/27/2012 to replace incorrect figure versions included during production

Evolutionary Trade-Offs, Pareto Optimality, and the Geometry of Phenotype Space

O. Shoval,[1] H. Sheftel,[1] G. Shinar,[1] Y. Hart,[1] O. Ramote,[1] A. Mayo,[1] E. Dekel,[1] K. Kavanagh,[2] U. Alon[1]*

[1]Department of Molecular Cell Biology, Weizmann Institute of Science, Rehovot, Israel.

[2]Biology Department, University of Massachusetts Dartmouth, Dartmouth, MA, USA.

*To whom correspondence should be addressed. E-mail: uri.alon@weizmann.ac.il

Biological systems that need to perform multiple tasks face a fundamental trade-off: a given phenotype cannot be optimal at all tasks. Here we ask how trade-offs affect the range of phenotypes found in nature. Using the Pareto front concept from economics and engineering, we find that best-trade-off phenotypes are weighted averages of archetypes—phenotypes specialized for single tasks. For two tasks, phenotypes fall on the line connecting the two archetypes, which could explain linear trait correlations, allometric relationships, as well as bacterial gene-expression patterns. For three tasks, phenotypes fall within a triangle in phenotype space, whose vertices are the archetypes, as evident in morphological studies including Darwin's finches. Tasks can be inferred from measured phenotypes based on the behavior of organisms nearest the archetypes.

Consider a biological system whose phenotype is defined by a vector of traits, v. Traits considered here are quantitative measures such as bird beak length, and not genetic traits such as DNA sequences. The space of all phenotypes is called the morphospace. Most theories of natural selection maximize a specific fitness function $F(v)$, resulting in an optimal phenotype, usually a point in morphospace. This approach has several limitations: first, the fitness function is often unknown. Second, in many cases organisms need to perform multiple tasks that all contribute to fitness (*1*); thus, fitness is an increasing function of the performance at all tasks $F(P_1(v),...,P_k(v))$, where $P_i(v)$ is the performance at task *i*. The best phenotype for one task is usually not the best for other tasks- resulting in a trade-off situation. Maximizing fitness is thus a multi-objective optimization problem (*2–5*).

To address this we employ the Pareto front concept (*6*), used in engineering and economics to find the set of designs that are best trade-offs between different requirements. Consider two phenotypes v and v'. If v' is better at all tasks than v, the latter will be eliminated by natural selection (Fig. 1A). Repeating this for all possible phenotypes, one remains with the Pareto front: the set of phenotypes which cannot be improved at all tasks at once. The Pareto front describes all optima for all conceivable fitness functions that are increasing functions of the performance in each task. Which of the phenotypes on the front is selected depends on the relative contributions of each task to the organisms' fitness in its natural habitat, provided that evolution has had sufficient time and genetic variance to reach the predicted point.

The Pareto front is typically a small region of morphospace. This may explain the long-standing observation that most of morphospace is empty (*7*): phenotypes such as animal shapes found in nature fill only a small fraction of morphospace.

We next calculate the Pareto front in morphospace. This requires two assumptions (which will be relaxed below). (i) Each performance function is maximized by a single phenotype. The phenotype that is best at task *i* will be called the *archetype* for task *i*, denoted v_i^*. (ii) Performance decreases with distance from the archetype (Fig. 1B). By distance we mean a metric based on an inner product norm, such as Euclidean distance (mathematically, $P_i(v)=P_i(d_i)$, where $d_i=(v-v_i^*)\,M\,(v-v_i^*)$, and M is a positive-definite matrix; Euclidean distance $d_i=(v-v_i^*)^2$ is when $M=I$). For two tasks, geometric considerations show that the Pareto front is the line segment that connects the two archetypes (Fig. 1C). This is because any point off the line segment is farther from both archetypes than its projection on the line - thus points off the line have lower performance at both tasks and hence lower fitness, and will be selected against. The position of a phenotype on the line relates to the relative importance of the two tasks in the habitat in which the organism evolved: the closer to an archetype, the more important that task (Fig. 1C inset, (*8*)).

The case of a trade-off between two tasks may explain the widespread occurrence of linear relations between traits (*2, 9, 10*). As an example, the area proportions of the molar teeth

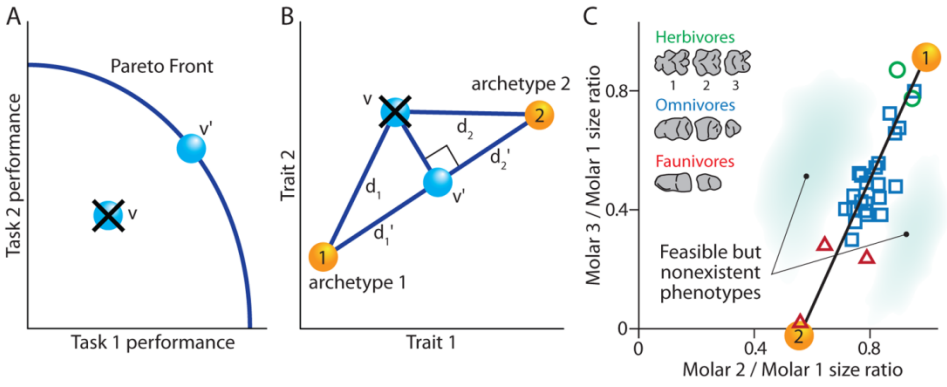

Fig. 1. A. The Pareto front (best trade-offs) is what remains after eliminating (crossed-out symbol) all feasible phenotypes *v*, that are dominated on all tasks by other feasible phenotypes *v'*. **B.** The two archetypes v_1^* and v_2^* in morphospace maximize performance in tasks 1 and 2. Phenotype *v* is farther from both archetypes than *v'*, its projection on the line segment that connects the archetypes. Thus *v* has lower performance than *v'* in both tasks, hence lower fitness. Eliminating all such points *v*, one remains with the Pareto front: the line segment connecting the two archetypes (unlike 1A, axes are traits not performances). **C.** The area ratios of rodent molar areas show a linear relationship (*11*). Most of morphospace is empty. Herbivores (circles), carnivores (triangles) and omnivores (squares) are indicated.

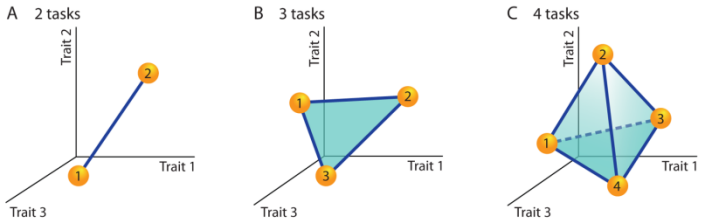

Fig. 2. Pareto front geometry. **A.** Two tasks form a line **B.** Three tasks form a triangle. **C.** Four tasks form a tetrahedron. If only some relevant traits are measured and others are not, lines and triangles should still be found, because a projection of a convex hull on a subspace is still a convex hull (*8*). The distribution of points along the front depends on the second derivative of the performance and fitness functions (*8*).

of 29 rodent species show an approximately linear relationship (*11*) (Fig. 1D). Species are distributed along the line according to their diet: herbivores at one end, carnivores at the other, and omnivores in the middle. Thus the archetypes correspond to the ends of the observed line segment: a herbivore archetype with equal-sized molars, and a carnivore archetype with molars in the ratio 2:1:0. Omnivore molars are weighted averages of these archetypes. As in many morphological studies, the traits here are normalized to account for organism size: since all molar areas scale with size, taking the ratio of molars removes the effect of organism size variation (*8*). Additionally, the present theory might explain cases of allometry, when the proportions of traits depend on total organism size (*9, 10*). In some cases allometric relations behave as power laws, observed as lines in logarithmic plots, predicted when the performance decays with a metric that is a function of the log of the traits (*8*). Other explanations for allometric relations include scaling laws for metabolic transport (*12*), and physical or developmental constraints (*10, 11*).

For more than two tasks, the Pareto front is the full polygon or polyhedron whose vertices are the archetypes, Fig. 2 (or, equivalently, the convex hull of the archetypes, defined as the set of all points that are weighted averages of the archetypes: $v = \sum_{i=1}^{k} \theta_i v_i^*$ with weights

$$\theta_i = \frac{\partial F}{\partial P_i}\frac{\partial P_i}{\partial d_i} \Big/ \sum_{j=1}^{k} \frac{\partial F}{\partial P_j}\frac{\partial P_j}{\partial d_j}.$$

Weights sum to one $\sum_{i=1}^{k} \theta_i = 1$, and are positive $\theta_i > 0$ because fitness increases with performance $\partial F / \partial P_i > 0$ and performance decreases with distance from its archetype $\partial P_i / \partial d_i < 0$ (*8*)). For three tasks, the Pareto front is the full triangle whose vertices are the three archetypes. In this case, because a triangle defines a plane, even high dimensional data on many traits is expected to collapse onto two dimensions. The closer a point is to one of the vertices of the triangle, the more important the corresponding task is to fitness in the organism's habitat.

We find evidence for such triangular suites of variation in several classical studies of animal morphology and evolution. In these studies, there was no theory to explain why the data resembles a triangle. The species near the vertices of the triangles have distinct behavior that suggests which task is optimized by each archetype (Fig. 3A-C). A triangle is found in the study of Grant and colleagues on Darwin's Finches (*13*) (Fig. 3A). Measurements of five beak and body traits (five dimensional morphospace) fall on a two dimensional plane: two principal components - related to body size and beak shape - account for 99% of the variation (*8*). On this plane, the data falls within a triangle ($p<10^{-4}$, according to a statistical test of triangularity, Fig. 4A inset (*8, 14*)). The triangle suggests three archetypes, one at each vertex. The species near the archetypes suggest which tasks may be optimized by each archetype, in this case tasks connected with diet: (1) probing for insects and nectar (long beak, cactus finch), (2) crushing hard large seeds (thick beak, large ground finch) and (3) crushing small soft seeds (small beak, small ground finch). Intermediate finch species perform a combination of these tasks (*8*).

We also noted a triangle-shaped suite of variation in E.O. Wilson's study of leaf cutter ants (*15*) (Fig. 3B, $p<10^{-4}$ (*8, 14*)). The three archetypes are associated with nursing/gardening, foraging outside the nest, and soldiering. Intermediate ants perform a combination of these tasks. Additionally, Norberg and Rayner's study of bat wings (*16*) (Fig. 3C, $p<3\cdot10^{-2}$, (*8, 14*)), shows a triangular pattern. Archetypes seem to be associated with eating insects in vegetation, hawking insects in the air far above vegetation, and eating large prey in vegetation.

The present considerations might apply beyond animal morphology. For example, bacteria face a trade-off in partitioning the total amount of

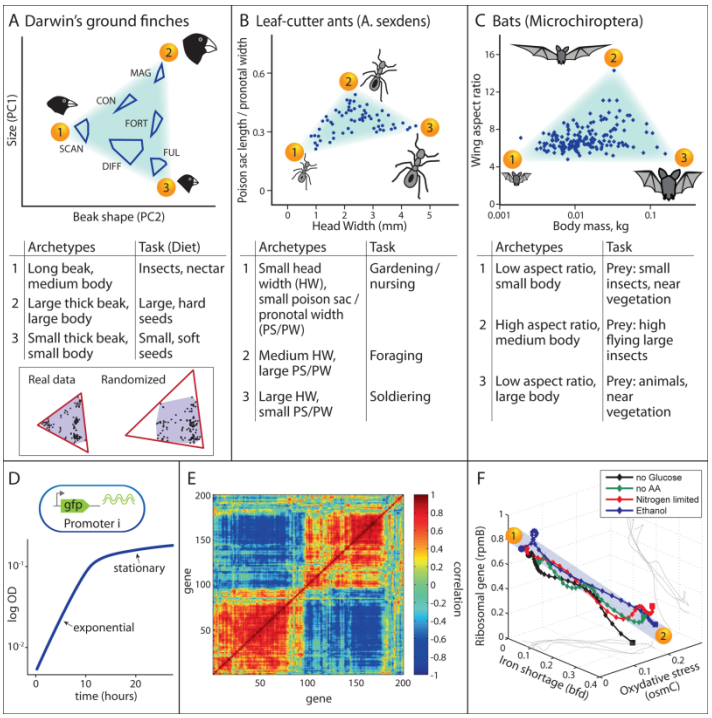

Fig. 3. Triangular suites of variation, and trade-offs in *E. coli* gene-expression. **A.** Darwin's ground finches (*13*). Axes correspond to size and beak shape. Polygons are boundaries of intra-species variation. See (*8*) for species definitions. Inset: Statistical test for triangularity. Define t-ratio as the ratio of the area of the minimal-area triangle (red) to the area of the convex hull of the data (purple). The p-value is the fraction of times that randomized data has larger t-ratio than the real data, based on 10^4 randomized datasets that preserve the statistics of each trait independently (*8*) **B.** Leaf-cutter ant (*15*): poison sac (pheromone gland that marks the trail) length (normalized to pronotal width) vs. head width. **C.** Bat (*microchiroptera)* wing aspect ratio vs. body mass (*16*). Archetypes and inferred tasks are listed below each figure. **D.** *E. coli* promoter activity was measured with fluorescent reporters (*18*). **E.** Clustered correlation matrix of the top 200 temporally varying genes. **F.** Percent of total promoter activity of three genes at different time points, in four different media conditions (*8*), as bacteria go from exponential phase (1) to stationary phase (2).

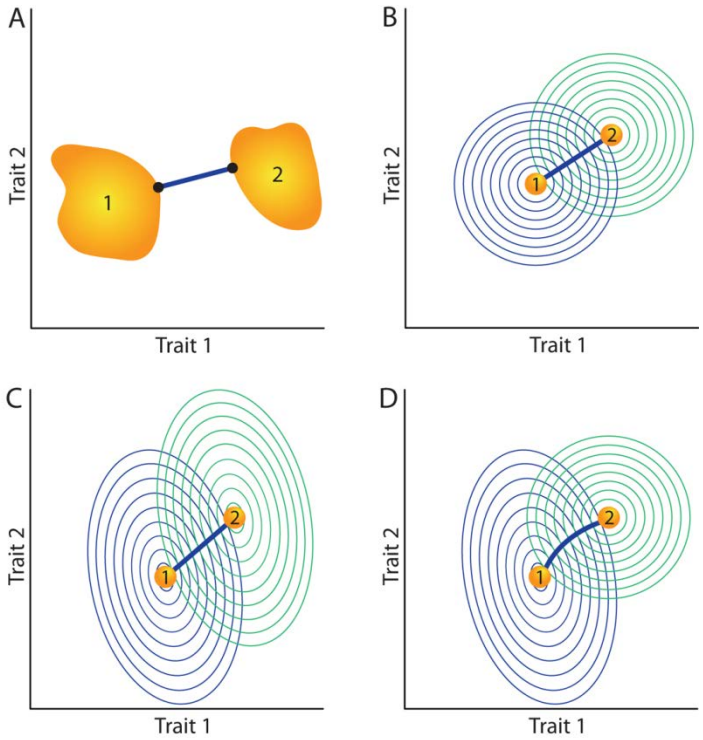

Fig. 4. A. Relaxing assumption (i): When performance is maximized in a region rather than a single point, the Pareto front is the line that connects the closest point in the region to the other archetypes (*8*). **B.** and **C.** When all performance functions decay with the *same* distance metric the Pareto front is a straight line. The front is the set of tangent points between equi-performance contours (*8*). **D.** Relaxing assumption (ii): When each performance function decays with a *different* metric (different elliptical contours) the front is slightly curved. Mean rms deviation from a straight line is 21%, averaged over ellipses of all orientations and major/minor axis ratios spanning a hundredfold range (*8*). For three tasks, triangles with curved edges are generally found.

proteins they can make at a given moment between the different types of proteins - in other words, how much of each gene to express. A given expression pattern can't be optimal, at the same time, to two different tasks such as rapid growth – which requires ribosomes - and survival – which requires stress response proteins (*17*). Thus, the theory predicts that gene expression patterns fall on low dimensional Pareto fronts, whose vertices are archetypal expression patterns optimal for a single task.

We tested this hypothesis on *E. coli* gene expression (Fig. 3D). The activity of 1,600 promoters was tracked using fluorescent reporters as bacteria grew from exponential to stationary phase (*18*) (Fig. 3E, (*8*)). Activity was normalized by the summed activity of all promoters at each time point, to represent the instantaneous allocation of transcription resources. The top 200 temporally varying promoters, account for 96% of the total temporal variation, and control genes in two main families (*8*): growth genes (ribosomes, transcription and translation), and stress/survival genes (oxidative stress, etc.). This high-dimensional dataset falls, on a line (Fig. 3F, $p<10^{-4}$ (*8*), fig. S10). At one end expression is devoted mostly to growth genes (exponential phase, archetype 1), and at the other end expression is devoted primarily to stress/survival genes (stationary phase, archetype 2). The expression program gradually moves along the line from archetype 1 to 2 as time goes by. The instantaneous allocation at each time point is, to a good approximation, a weighted average of two archetypal expression programs: growth and survival. Similar analysis may explain low-dimensional patterns in gene expression measurements in bacteria (*19*) and cancer cells (*20*).

Relaxing the assumptions (i) and (ii) above generally preserves the topology of the Pareto front, with mildly curved lines instead of straight edges, but nevertheless with distinct vertices that can be related to archetypes (Fig. 4, (*8*)).

The present theory addresses traits which have a trade-off. If a trade-off does not exist, trait values can vary independently. Observed phenotypes in this case may fill an uncorrelated cloud in morphospace (*8*).

It is interesting to note that variation in traits within a population in a given species often fall on the same line as variations between species - a phenomenon called 'evolution along genetic lines of least resistance' (*21*). This can be explained by the present framework: Variation within a species reflect the range of habitats it inhabits, each with differential importance of the tasks. Thus, populations should be distributed on the same Pareto front as different species facing the same tasks.

Finally, we note that Pareto optimality need not be the only or generic explanation for low dimensionality and lines/triangles in biological data. It may work for some examples and not others, especially if there are biological constraints other than natural selection at play. The following experimental tests can refute the theory in a specific example: (a) A point in the middle of the front has higher performance in one of the tasks than a point close to the relevant vertex (note that this might also imply that different tasks are at play). (b) A mutant can be found that has higher performance at all tasks than existing phenotypes. Both of these tests require measuring performance (*7*, *13*) - but not the more difficult task of measuring fitness. (c) Laboratory evolution experiments can follow a mutant that is off the Pareto front (has lower performance in all tasks than the wild type), under conditions in which all tasks are required. Provided with sufficient genetic variation, the mutant is predicted to evolve phenotypes closer to the front.

References and Notes

1. S. J. Arnold, Morphology, Performance and Fitness. *Am. Zool.* **23**, 347 (1983).
2. G. F. Oster, E. O. Wilson, *Caste and Ecology in the Social Insects* (Princeton University Press, 1979).
3. K. D. Farnsworth, K. J. Niklas, Theories of optimization, form and function in branching architecture in plants. *Funct. Ecol.* **9**, 355 (1995). doi:10.2307/2389997
4. H. El Samad, M. Khammash, C. Homescu, L. Petzold, Optimal performance of the heat-shock gene regulatory network, *Proc. 16th IFAC World Congress* (2005).
5. M. C. Kennedy, Functional–structural models optimize the placement of foliage units for multiple whole-canopy functions. *Ecol. Res.* **25**, 723 (2010). doi:10.1007/s11284-009-0658-6
6. R. E. Steuer, Multiple criteria optimization: theory, computation, and application (Wiley, 1986).
7. G. R. McGhee, The geometry of evolution: adaptive landscapes and theoretical morphospaces (Cambridge University Press, 2007).
<foot>8. SOM, Supporting Online Material, .</foot>
9. S. J. Gould, Allometry and size in ontogeny and phylogeny. *Biol. Rev. Camb. Philos. Soc.* **41**, 587 (1966). doi:10.1111/j.1469-185X.1966.tb01624.x Medline
10. C. P. Klingenberg, Evolution and development of shape: integrating quantitative approaches. *Nat. Rev. Genet.* **11**, 623 (2010). Medline
11. K. D. Kavanagh, A. R. Evans, J. Jernvall, Predicting evolutionary patterns of mammalian teeth from development. *Nature* **449**, 427 (2007). doi:10.1038/nature06153 Medline
12. G. B. West, J. H. Brown, B. J. Enquist, A general model for the origin of allometric scaling laws in biology. *Science* **276**, 122 (1997). doi:10.1126/science.276.5309.122 Medline
13. P. R. Grant, I. Abbott, D. Schluter, R. L. Curry, L. K. Abbott, Variation in the

size and shape of Darwin's finches. *Biol. J. Linn. Soc. Lond.* **25**, 1 (1985). doi:10.1111/j.1095-8312.1985.tb00384.x
<foot>14. Software that analyzes data in terms of triangles and their significance, and suggests archetype trait values, is available for download at www.weizmann.ac.il/mcb/UriAlon.</foot>
15. E. O. Wilson, Caste and division of labor in leaf-cutter ants (Hymenoptera: Formicidae: Atta). *Behav. Ecol. Sociobiol.* **7**, 143 (1980). doi:10.1007/BF00299520
16. U. M. Norberg, J. M. V. Rayner, Ecological Morphology and Flight in Bats (Mammalia; Chiroptera): Wing Adaptations, Flight Performance, Foraging Strategy and Echolocation. *Philos. Trans. R. Soc. Lond. B Biol. Sci.* **316**, 335 (1987). doi:10.1098/rstb.1987.0030
17. T. Nyström, Growth versus maintenance: a trade-off dictated by RNA polymerase availability and sigma factor competition? *Mol. Microbiol.* **54**, 855 (2004). doi:10.1111/j.1365-2958.2004.04342.x Medline
18. A. Zaslaver *et al*., Invariant distribution of promoter activities in Escherichia coli. *PLOS Comput. Biol.* **5**, e1000545 (2009). doi:10.1371/journal.pcbi.1000545 Medline
19. M. Scott, C. W. Gunderson, E. M. Mateescu, Z. Zhang, T. Hwa, Interdependence of cell growth and gene expression: origins and consequences. *Science* **330**, 1099 (2010). doi:10.1126/science.1192588 Medline
20. N. Geva-Zatorsky *et al*., Protein dynamics in drug combinations: a linear superposition of individual-drug responses. *Cell* **140**, 643 (2010). doi:10.1016/j.cell.2010.02.011 Medline
21. D. Schluter, Adaptive Radiation Along Genetic Lines of Least Resistance. *Evolution* **50**, 1766 (1996). doi:10.2307/2410734
22. C. B. Barber, D. P. Dobkin, H. Huhdanpaa, The quickhull algorithm for convex hulls. *ACM Trans. Math. Softw.* **22**, 469 (1996). doi:10.1145/235815.235821
23. V. Klee, M. C. Laskowski, Finding the smallest triangles containing a given convex polygon. *J. Algorithms* **6**, 359 (1985). doi:10.1016/0196-6774(85)90005-7
24. O. Campàs, R. Mallarino, A. Herrel, A. Abzhanov, M. P. Brenner, Scaling and shear transformations capture beak shape variation in Darwin's finches. *Proc. Natl. Acad. Sci. U.S.A.* **107**, 3356 (2010). doi:10.1073/pnas.0911575107 Medline
25. P. R. Grant, *Ecology and evolution of Darwin's finches* (Princeton University Press, 1999).
26. S. J. Millington, P. R. Grant, Feeding ecology and territoriality of the Cactus Finch Geospiza scandens on Isla Daphne Major, Galapagos. *Oecologia* **58**, 76 (1983). doi:10.1007/BF00384545
27. P. R. Grant, B. R. Grant, Evolution of character displacement in Darwin's finches. *Science* **313**, 224 (2006). doi:10.1126/science.1128374 Medline
28. B. R. Grant, Selection on Bill Characters in a Population of Darwin's Finches: Geospiza conirostris on Isla Genovesa, Galapagos. *Evolution* **39**, 523 (1985). doi:10.2307/2408650
29. D. Schluter, P. R. Grant, Ecological Correlates of Morphological Evolution in a Darwin's Finch, Geospiza difficilis. *Evolution* **38**, 856 (1984). doi:10.2307/2408396
30. B. Holldobler, E. O. Wilson, *The Ants* (Belknap Press of Harvard University Press, ed. 1st, 1990).
31. J. S. Findley, D. E. Wilson, Observations on the neotropical disk-winged bat, Thyroptera tricolor spix. *J. Mammal.* **55**, 562 (1974). doi:10.2307/1379546 Medline
32. G. Neuweiler, Auditory adaptations for prey capture in echolocating bats. *Physiol. Rev.* **70**, 615 (1990). Medline
33. A. M. Hutson, Microchiropteran bats: global status survey and conservation action plan (IUCN, 2001).
34. D. Navarro, D. E. Wilson, Vampyrum Spectrum. *Mammal. Species* **184**, 1 (1982).
35. W. S. Hudson, D. E. Wilson, Macroderma gigas. *Mamm. Species* **260**, 1 (1986). doi:10.2307/3503920
36. A. Zaslaver *et al*., A comprehensive library of fluorescent transcriptional reporters for Escherichia coli. *Nat. Methods* **3**, 623 (2006). doi:10.1038/nmeth895 Medline
37. T. Bollenbach, R. Kishony, Resolution of gene regulatory conflicts caused by combinations of antibiotics. *Mol. Cell* **42**, 413 (2011). doi:10.1016/j.molcel.2011.04.016 Medline
38. Y. Savir, E. Noor, R. Milo, T. Tlusty, Cross-species analysis traces adaptation of Rubisco toward optimality in a low-dimensional landscape. *Proc. Natl. Acad. Sci. U.S.A.* **107**, 3475 (2010). doi:10.1073/pnas.0911663107 Medline
39. P. C. Wainwright, M. E. Alfaro, D. I. Bolnick, C. D. Hulsey, Many-to-One Mapping of Form to Function: A General Principle in Organismal Design? *Integr. Comp. Biol.* **45**, 256 (2005). doi:10.1093/icb/45.2.256 Medline
40. H. W. Kuhn, A note on Fermat's problem. *Math. Program.* **4**, 98 (1973). doi:10.1007/BF01584648
41. Lande, Natural selection and random genetic drift in phenotypic evolution. *Evolution* **30**, 314 (1976). doi:10.2307/2407703
42. M. Kimura, *The Neutral Theory of Molecular Evolution* (Cambridge University Press, 1985).
43. D. M. Raup, Geometric Analysis of Shell Coiling: General Problems. *J. Paleontol.* **40**, 1178 (1966).
44. J. Maynard Smith *et al*., Developmental Constraints and Evolution: A Perspective from the Mountain Lake Conference on Development and Evolution. *Q. Rev. Biol.* **60**, 265 (1985). doi:10.1086/414425
45. W. A. Frankino, B. J. Zwaan, D. L. Stern, P. M. Brakefield, Natural selection and developmental constraints in the evolution of allometries. *Science* **307**, 718 (2005). doi:10.1126/science.1105409 Medline
46. C. E. Allen, P. Beldade, B. J. Zwaan, P. M. Brakefield, Differences in the selection response of serially repeated color pattern characters: standing variation, development, and evolution. *BMC Evol. Biol.* **8**, 94 (2008). doi:10.1186/1471-2148-8-94 Medline

Acknowledgments: We thank N. Barkai, R. Milo, O. Feinerman, C. Tabin, J. Losos, M. Khammash, T. Dayan, and N. Ulanovski for discussion. UA holds the Abisch-Frenkel Professorial Chair; OS is an Azrieli Fellow. This work was supported by the Israel Science Foundation, and the European Research Council (FP7).

Supplementary Materials
www.sciencemag.org/cgi/content/full/science.1217405/DC1
Materials and Methods
Figs. S1 to S24
Table S1
References (*22*–*46*)

2 December 2011; accepted 6 April 2012
Published online 26 April 2012
10.1126/science.1217405